ORIGINAL ARTICLE

Prediction of autogenous shrinkage in concrete from material composition or strength calibrated by a large database, as update to model B4

Mohammad Rasoolinejad · Saeed Rahimi-Aghdam · Zdeněk P. Bažant

Abstract In modern concretes, the autogenous shrinkage, i.e., the shrinkage of sealed specimens, is much more important than it is in traditional concretes. It dominates the shrinkage of thick enough structural members even if exposed to drying. A database of 417 autogenous shrinkage tests, recently assembled at Northwestern University, is exploited to develop empirical predictive equations, which improve significantly those embedded in RILEM Model B4. The data scatter is high and the power law $(time)^{0.2}$ is found to be optimal for times ranging from hours to several decades of years, as the test data give no hint of upper bound. Statistics of data fitting yields the approximate dependence of the power law parameters on the water-cement and aggregate-cement ratios, cement type, additives such as the blast furnace slag and silica fume, and curing type and duration. Alternatively, the power law parameters can be reasonably well predicted from the compression strength alone. Since some database entries do not report all these composition parameters and others do not report the compressive strength, and since the concrete strength is often the only material property specified in design, two types of models are formulated—composition based, and strength based. Both are verified by statistical comparisons with individual tests, and optimized by nonlinear statistical regression of the entire database, so as to minimize the coefficient of variation of deviations from the data points normalized by the overall data mean. The regression is weighted so as to compensate for the bias due to crowding of data in the short-time range. Statistical comparisons with the prediction models in the JSCE code, Eurocode and CEB MC90-99 code (identical to *fib* Model Code 2010) show the present model to give significantly better data fits. Finally it is emphasized that, in presence of external drying and creep, accurate predictions will require treating the autogenous shrinkage as a consequence of pore humidity drop caused jointly by self-desiccation due to hydration and by moisture diffusion, and solving the time evolution of humidity profiles. The present model is proposed as an update for the autogenous shrinkage formula in model B4, although recalibration of the whole B4 would be needed.

Keywords Autogenous shrinkage · Swelling · Predictive model · Concrete composition · Concrete strength · NU database

M. Rasoolinejad · S. Rahimi-Aghdam
Graduate Research Assistant, Northwestern University, Evanston, IL, USA

Z. P. Bažant (✉)
McCormick Institute Professor and W.P. Murphy Professor of Civil and Mechanical Engineering and Materials Science, Northwestern University, 2145 Sheridan Road, CEE/A135, Evanston, IL 60208, USA
e-mail: z-bazant@northwestern.edu

1 Introduction

Although the design lifetimes of large concrete structures are typically required to exceed 100 years, recent studies of 69 large-span prestressed box-girder bridges document lifetimes of two to five decades [1–4]. The slabs in such bridges, as well as other structures, can be up to about 1 m thick, and in that case the cross section core will not suffer any drying for many decades [5–7]. The same is true for massive columns, geotechnical concrete structures, etc. This makes it possible for hydration and the associated autogenous shrinkage to proceed for the entire lifetime.

Recent studies also reveal that modern concretes with low water-cement ratios have a much higher autogenous shrinkage than the old ones; and that the hydration reaction, and thus also the autogenous shrinkage, can advance at pore humidities as low as 65% [6–8]. Therefore, for modern concretes, the autogenous shrinkage is much more important than for traditional ones, and is so for any thickness.

Because of the unfortunate ingrained habit of engineers to plot the test results in the linear time scale [9], it has been widely believed that the autogenous shrinkage reaches an upper bound within a few months. But data plots in the logarithmic time scale reveal that the hydration, and thus also the autogenous shrinkage, continues for decades, with no bound in sight. A bound must, of course, exist because the amount of reactants in hydration is finite, but it obviously lies beyond the times of interest for structural design.

The autogenous shrinkage, discovered in 1934 by Lynam [10], is defined as the volumetric strain of concrete due to hydration reaction, excluding the drying shrinkage, thermal dilatation and creep under applied stress [11–13]. Although the autogenous shrinkage has often been regarded as a direct result of hydration [14, 15], it has been shown [6, 16–20] to be caused by a decrease of relative humidity, Δh, in the pores, due to self-desiccation (which, in turn, is caused by hydration). The effect of Δh on autogenous shrinkage increment follows the same point-wise law as the shrinkage due to external drying [21, 22]. However, models reflecting this fact [6, 23–30] require sophisticated computer analysis.

Some researchers claim that the self-desiccation is hard to explain because cavitation that would nucleate new vapor bubbles in liquid water is next to impossible. True, but new bubbles are not needed. Self-desiccation merely enlarges the existing vapor space, pushing the capillary menisci into narrower pores.

For the normal concrete, the water-cement ratio is much higher than what is needed for the hydration reaction, and so the decrease of relative humidity, Δh, is small (about 3%). For this reason, the autogenous shrinkage has usually been neglected by designers [3]. But with increasing use of high strength concretes (HSC) and high performance concretes (HPC), which have a low water-cement ratio, the drop in relative humidity is significant (even by $> 30\%$), and thus correct estimation of autogenous shrinkage becomes important [12, 31].

The chemical reactions of hydration that cause self-desiccation begin as soon as the cement is mixed with water, and so the autogenous shrinkage begins before other deterioration processes come to play. The structural constraints often resist shrinkage and induce tensile stresses and cracks. The cause of early age cracking is usually the autogenous shrinkage [20, 32–36]. The aggregates enforce a constraint on the shrinkage [37] of hardened cement paste and thus generates micro-cracks. Although these microcracks cannot cause failure, they can greatly decrease strength and durability [38].

Here we aim at a simple model to predict the autogenous shrinkage at no moisture exchange, as in sealed specimens, which is what suffices for a general practical prediction model such as B4 [3]. The present goal is to improve the model now embedded in B4 [3], and to validate it by comparisons with the relevant individual tests, and with a large experimental database of 417 tests assembled at Northwestern. Statistical comparisons will be made. They will demonstrate superiority to the existing models in the JSCE code [39], the Eurocode [40] and the CEB MC90-99 code [41] (identical to *fib* Model Code 2010 [42]). Replacement of the self-desiccation formulae of model B4 with the present formulae helps, but better the entire B4 should be recalibrated.

2 Review of previous studies

Neville [43] concluded that the type of cement and its fineness affect the autogenous shrinkage. The studies of Swayze [44] and of Bennett and Loat [45] showed

that finer cement grains lead to a higher shrinkage in cement paste but not necessarily in concrete. Miyazawa and Tazawa [46] performed test to assess the effect of cement type, considering ordinary Portland cement (N), moderate-heat Portland cement (M), high-early-strength Portland cement (H), and low-heat Portland cement (L). Based on their tests, they proposed cement type factors as listed in Table 1. A statistical study of the NU database confirms the effect of cement type and indicates similar cement type factors as Miyazawa and Tazawa study on cements of similar types as defined in the CEB Model Code (SL, N, R, RS). The Model Code defined the cement types as R-normal, RS-rapid hardening, and SL-slow hardening which is also used in model B4 (see [3] under Eq. 43).

Many tests have been done in order to clarify the effect of supplementary cementitious materials on autogenous shrinkage. Tazawa and Miyazawa's tests [47] showed that adding silica fume to the concrete mix increases the autogenous shrinkage. While most of studies [48–52] confirm this conclusion, there are nevertheless some that indicate no effect of silica fume. Some studies suggest that adding silica fume can change pore distribution [53–55] which can affect autogenous shrinkage.

Adding slag to the concrete generally increase the autogenous shrinkage [47, 56–58], although some tests [59, 60] show the opposite. The change in autogenous shrinkage might be related to the filling of nanopores by slag [61], as well as silica fume. In the case of concrete with fly ash, there are again discrepancies in experimental results. Some studies indicate that adding fly-ash reduces the autogenous shrinkage [60, 62] while others show the opposite [63]. These discrepancies may be caused by differences in defining w/c or the mass ratio of water-cementitious binders. In the NU database, these two parameters are not distinguished, because of insufficient information. Also, the time reference in most of shrinkage tests is arbitrary, which may produce such inconsistencies.

Neville [43] observed that the modulus of elasticity of the aggregates, E_{ag}, greatly affects the shrinkage. Hobbs [64] proposed an equation for the effect of aggregate type and content. A higher E_{ag} restrains the overall deformation, but this is significant only for very high aggregate to cement ratio, close to compact aggregate packing. For a lower a/c, relative deformation between aggregate pieces and cement paste creep can increase the autogenous shrinkage. It has been shown that the aggregate with rough surface can reduce the shrinkage [65]. So, the aggregate shape and its grading can also have effect. The type of aggregate was reported for only about half of the tests in the NU database, and no correlation to autogenous shrinkage transpired. More test data are needed for more comprehensive conclusion.

Temperature affects greatly the hydration reaction [66–68]. Elevated temperature increases the hydration rate and thus the autogenous shrinkage, especially at early age [69]. Some experimentalists [70, 71] used the maturity concept to predict the temperature effect on autogenous shrinkage, while many others [67, 72–77] refuted its applicability. The concept of equivalent age $\bar{t}$ has been adopted in models B3 and B4 [3, 78] and can be used for the present model as well. Unfortunately, most testing was done either at room temperature or with no temperature control.

The effect of the curing type is significant but, unfortunately, ignored by most models. One obvious property is that the stiffness increases during curing, and this increase tends to inhibit shrinkage at a later time. Collins tests show the moist-cured specimens to shrink less [79], in proportion to the curing time. The early studies either ignored the autogenous shrinkage during curing or subtracted it from the observed total autogenous shrinkage.

3 Northwestern creep and shrinkage database

After the discovery of concrete shrinkage, by H.L. Le Chatelier in Paris in 1887 and concrete creep by W.K. Hatt at Purdue University in 1907, a vast number of creep and shrinkage tests has been performed around the world. The first comprehensive creep and

Table 1 Cement type factor

Cement type (CEB equivalent)	N (R)	H (RS)	M (N)	L (SL)
Cement type factor (k_γ)	1.0	1.2	0.85	0.4

shrinkage database was gathered at Northwestern University in 1978. It comprised about 400 creep tests and about 300 shrinkage tests [80, 81]. This database was expanded in 1993 to a RILEM database with 518 creep and 426 shrinkage tests [81], and was used to develop RILEM Model B3 [78]. While working on Model B4, the database expanded to 1433 creep and 1827 shrinkage tests with 61,045 data points [82]. The database can be freely downloaded from http://www.civil.northwestern.edu/people/bazant/ or http://www.baunat.boku.ac.at/creep.html.

Many tests in the database, unfortunately, did not follow the optimum tests procedure, and some of them were performed on old concretes. Nevertheless, with judicious evaluation, these tests can still give useful information, especially for long-term (multi-decade) creep and shrinkage, the tests of which are scant [83]. Until they can be replaced with better tests, their use is inevitable.

While both short-term and long-term behaviors of concrete are important for safe structural design, most of the data points are crowded at short ages, short drying times and short-load durations [83]. Only 5% of data points pertain to durations of more than 6 years and only 3% for 12 years or more. Multi-decade autogenous shrinkage tests include only the 23-years tests of Troxell et al. [84] and 30-years tests of Brooks [85] (although the environmental controls of the latter were compromised, to an unknown extent, at 6 years).

The database in the original format is not suitable for statistical regression. The conditional coefficient of variation shows the data to be strongly heteroscedastic [81]. So the statistics of prediction model deviations for the data should be based on a proper unbiased statistical method which makes the data homoscedastic. This is achieved by giving equal weights to equal intervals on log-time, and eliminates bias due to data crowding at short time. This is attained by assigning weights inversely proportional to the number of data points in equal intervals of log-time. These corrections of statistical bias have been approximated by the data evaluations at Northwestern University since 1978. They have been systematically introduced by [86], presented in detail in [87], and strictly followed in the present study.

4 Autogenous shrinkage model

Imperfections in recording the exact setting time, in specimen sealing, in temperature control and in avoidance of mechanical constraints, as well as unrecorded curing procedure, etc., contaminated the existing test data. So, it is inevitable to study many tests to uncover the basic trends. All of the tests from the Northwestern University (NU) database satisfying the following necessary criteria have been considered in statistical evaluation:

1. The test includes at least 3 data points.
2. The test lasts for at least 1 week.
3. The specimen seal is not suspected to have leaked.
4. No reactive aggregate has been used [88, 89].

These criteria reduced the number of usable autogenous shrinkage tests from 417 to 340.

4.1 Functional form

Up to now, most of the autogenous shrinkage models assumed the hydration reaction to stop early, in less than 3 months. That is why the autogenous shrinkage in most existing formulae terminates soon with a horizontal asymptote. However, recent theoretical studies confirm that, at high pore humidity, the hydration reaction continues for decades, and all the long-term test data (plotted in log-time) confirm it [85, e.g.] (Fig. 1). Even during the development of model B4, it was noticed that test data does not show asymptotic bound. In fact, it was stated that "no test data with long enough duration exist to confirm it" [90]. The misconception arose from the misleading ingrained habit of plotting the creep and shrinkage data in a linear time scale. To reveal the long-term trend, as well as short-term, a logarithmic scale is required.

Unfortunately, not enough long-term tests are available. But the limited long-term test data that exist indicate the autogenous shrinkage strain to grow as a power law with exponent about 0.2; 32 tests in NU database lasted at least 10 years, and they all showed the power law trend, with no evidence of terminal bound. Most of the other tests, with mid-term and short-term durations, conform to the power law well. Besides, any law with a bound would require more parameters. From the physical viewpoint, the fact that

Fig. 1 Shrinkage curves of Brooks test data in **a** log–log and **b** semi-log scale
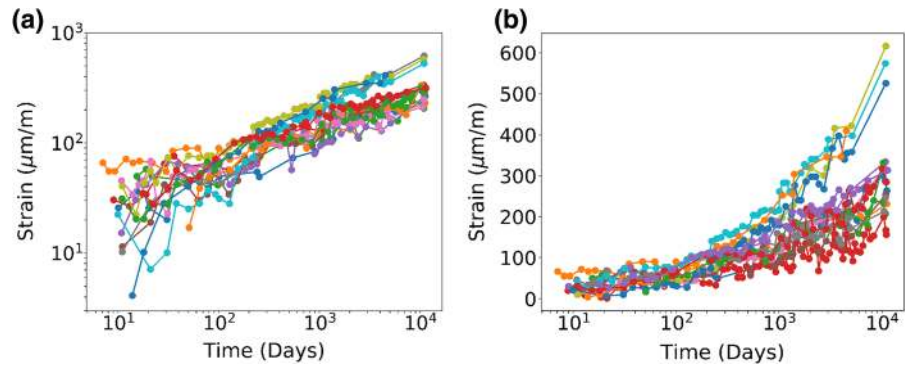
no characteristic time at which the trend would change is known implies that the law of long-time autogenous shrinkage must be self-similar, and this can be true only for a power law. There exists, of course, no evidence for a 100 years lifetime, but assuming a final bound would be an unconservative hypothesis. Also, introducing a final asymptote would make the functional form more complicated, for no reason.

There are two physical reasons for multi-decade growth without any bound. One is that the hydration reaction proceeds much longer than assumed until recently. The remnants of reacting anhydrous grains are surrounded by growing shells of C-S-H which delay more and more the access of water molecules to these grains [6, 91]. This causes the hydrations reaction to proceed, at a declining rate, for decades, provided the pore humidity does not drop too low (in drying specimens, the autogenous shrinkage is, of course, appears to be bounded, but this is beyond the scope of this study).

The second reason is the likelihood of local domains of cement paste undergoing creep driven by stresses in pore water. The reduction of relative vapor pressure due to hydration causes an increase in capillary tension and a decrease in disjoining pressure in hindered adsorbed water in nanopores [20, 56, 92, 93]. These stress changes in the pore water must be locally balanced by compressive stresses in the solid phase. They must cause creep, although doubtless less creep than an externally applied pressure because they are not uniform, compressing only dispersed localized nano-volumes [91, 94]. This may be captured by Biot coefficient of poromechanics. Because there is no external load, this localized creep is manifested as shrinkage, and its nonuniformity may cause microcracks. This localized

creep would remain even if pore humidity drop would stop hydration.

4.2 Model calibration

A look at the curves of observed data suggests describing the evolution of autogenous shrinkage by a power function:

$$\epsilon_{au} = k_\gamma k_s C \left(\frac{t}{1 \text{ day}} \right)^n \tag{1}$$

where t is the time (or age, measured from the moment of set); prefactor C and exponent n are empirical dimensionless parameters depending on the type of concrete; k_γ is cement type factor as listed in Table 1 and k_s takes into account the effect of additives. Figure 2a reveals that n and C are mutually correlated and depend on the aggregate-cement ratio (a/c). If a/c is increased while n is kept constant, C needs to be decreased, which further implies that an increase in a/c causes overall the autogenous shrinkage to decrease.

A plot of n versus log C yields a set of data points that can be reasonably well fitted with straight lines of nearly the same slopes in semi-log scale (Fig. 2a), mutually shifted as a function of a/c; hence

$$n = p + q \ln C \tag{2}$$

where p and q are empirical parameters depending on aggregate to cement ratio (a/c). The following functions give good data fits:

$$p = 1.2 - 0.1(a/c) \quad q = -0.14 + 0.005(a/c) \tag{3}$$

Examination of test data suggests that prefactor C decreases as water-cement ratio (w/c) and aggregate to cement ratio (a/c) increase (see the 3D plots in Fig. 2b). This result conforms to the fact that
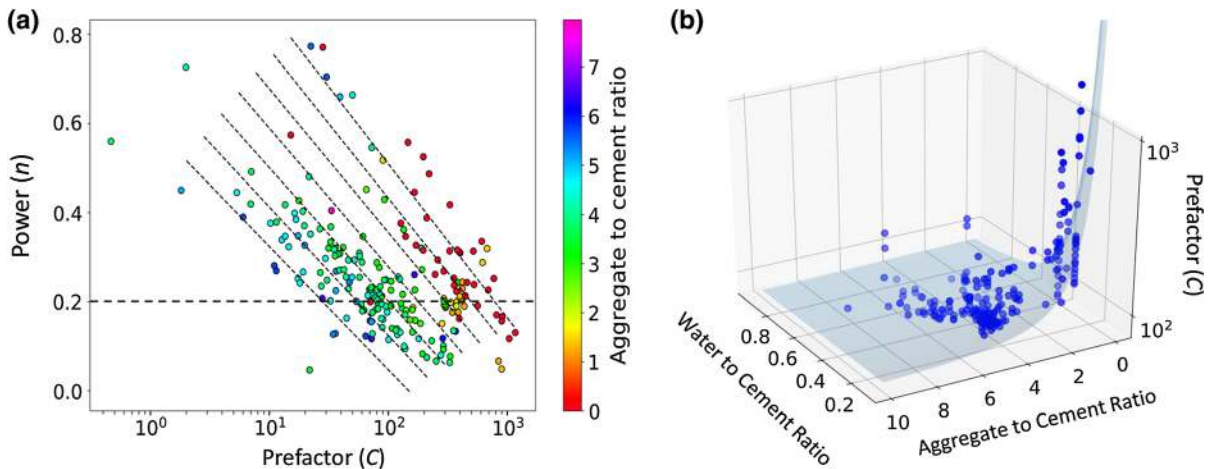
Fig. 2 Power law calibration based on concrete composition (**a**) prefactor and power correlation (**b**) prefactor calibration

autogenous shrinkage decreases as these two increase [20, 37, 47, 52], while the effects of the cement and admixtures types are weak. Several functional forms for C have been considered, and the following equation is proposed based on minimizing the sum of squared errors compared to the database (from which several outliers were omitted):

$$C = \frac{100}{(w/c)^{2.5} + (\frac{a/c}{10})^{1.5}} \quad (4)$$

This equation is applicable to the *w/c* ratio in the range of 0.2–0.8 and *a/c* ratio from 0 to 7. The aggregate to cement ratio in this formula includes both coarse and fine aggregates.

Statistical analysis of the NU database shows the silica fume tends to increase the autogenous shrinkage, especially at early age. The data of Mazloom et al. [95] clearly shows such an effect. The results indicate that the autogenous shrinkage increases on the average by 3% for every percent of increases in silica to cement ratio, as long as the cement replacement remains less than 20%. For higher percentages, the database information is insufficient.

Prefactor C shows an increase by almost 2% for every 1% increase in the slag-to-cement ratio (by weight). The limited data on concrete containing fly ash does not show any effect on the autogenous shrinkage. Adding superplasticizer can cause either increase or decrease, depending on the dosage and chemical composition.

4.3 Delayed start of measurement

The shrinkage measurements usually started not right after casting, but after the curing (wet or sealed). But the hydration reaction begins as soon as the cement is mixed with water. If the measurements begin later than at the moment of set, the initial part of shrinkage curve should be subtracted to come up with correct prediction (Fig. 3a). So the shrinkage after sealed curing should be calculated as

$$\epsilon_{au}(t - t_s) = \epsilon_{au}(t) - \epsilon_{au}(t_s) \quad (5)$$

where t = time (in days) after set and t_s = time at which measurement started.

4.4 Swelling simultaneous with autogenous shrinkage

Based on the arguments advanced in [91] and in more detail in [7], the hydration always causes expansion, and what causes autogenous shrinkage is the self-desiccation, which counteracts the expansion but often does not prevail at the beginning. The expansion is caused by growing diameters of C-S-H shells surrounding the remnants of anhydrous cement grains. The growth of adjacent shells in contact pushes each other apart, developing contact pressure akin to crystallization pressure or disjoining pressure.

Formation of the ettringite (calcium sulfoaluminate), which is also expansive, was previously suggested as a possible cause of the initial swelling [91], and may indeed contribute. But it cannot replace the
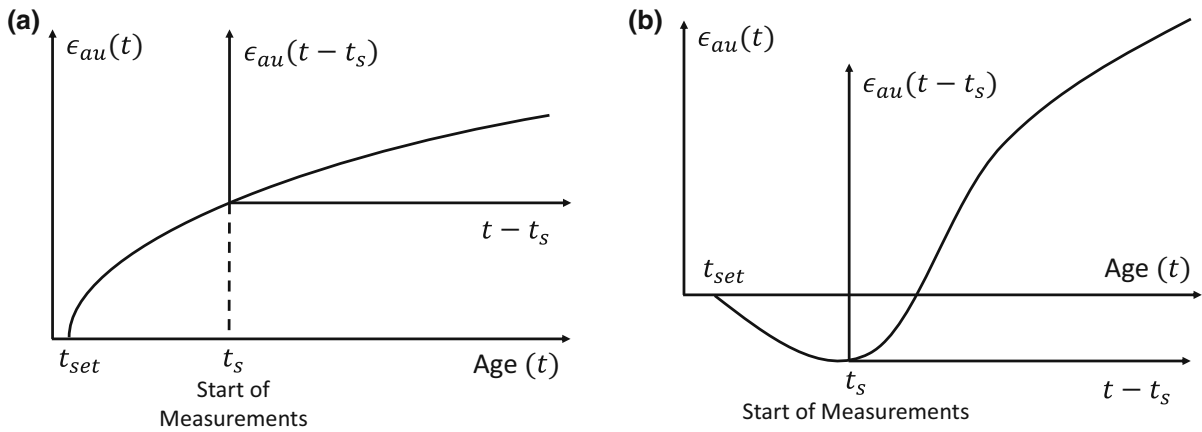
Fig. 3 Effect of the lag in measurements

growth effect of C-S-H shells which is needed to explain and model a broad range of other phenomena [7].

What actually drives autogenous shrinkage is a reduction of relative humidity h in the pores caused by self-desiccation [7, 91], which itself is caused by a loss of pore water due to hydration. In the case of curing underwater immersion, water diffuses into the specimen, offsetting the humidity reduction near the specimen surface due to self-desiccation. This explains why for wet curing the swelling is stronger for sealed curing.

Consequently, the total deformation in autogenous shrinkage tests is actually the sum of the 'pure' autogenous shrinkage and the swelling, which has the opposite sign. Depending on their magnitudes, the initially observed deformation may still be shrinkage, but more often swelling, later transiting into shrinkage. The swelling happens for both sealed curing and wet curing.

Both the autogenous shrinkage and swelling contribute to the observed deformation, making it difficult to identify the effect of each contribution individually. Separation of both contributions would require supplementing the fundamental theory in [96] by new special tests and optimizations. For the early age concrete, we simply assume the autogenous shrinkage to hold its functional form and to be superposed with a swelling function in the form of a power-law;

$$\epsilon_{sw} = -k\, t^{0.2} \quad \text{(for } t < t_c) \tag{6}$$

The swelling function reaches long term horizontal asymptote after the specimen gets sealed and the external supply of water stops;

$$\epsilon_{sw} = -k\, t_c^{0.2} - \frac{k\,(t^{0.2} - t_c^{0.2})}{1 + (t - t_c)^{0.2}} \quad \text{(for } t > t_c) \tag{7}$$

Here t is the time after the set and t_c is the time of wet curing (in days). If the concrete is sealed right after it is cast, $t_c = 0$. Due to lack of data, k is assumed; $k = 250$. If measurements start at a later time t_s (Fig. 3), only the increment is used:

$$\epsilon_{sw}(t - t_s) = \epsilon_{sw}(t) - \epsilon_{sw}(t_s) \tag{8}$$

For structural analysis, consider that ϵ_{sw} begins at the time of set, i.e., $t_s = 0$. For the lab specimen for which the measurements started only after curing, use $t_s = t_c$.

While Eq. (7) could successfully capture swelling in some cases, it increases the overall CoV of errors from 0.36 to 0.39. Adding the swelling reduces the predicted early-age shrinkage such that the model cannot capture the mean of data anymore (Fig. 4). Factor k could be a function of the water-cement and aggregate-cement ratios as well as the chemical composition of the cement and its fineness. The curing method might also have an effect as the surface emissivity for water and fog might be different. The water diffusion in wet cured specimen makes the swelling depend on the specimen size as well. Figure 5 shows that the data spread is broader at early age. One
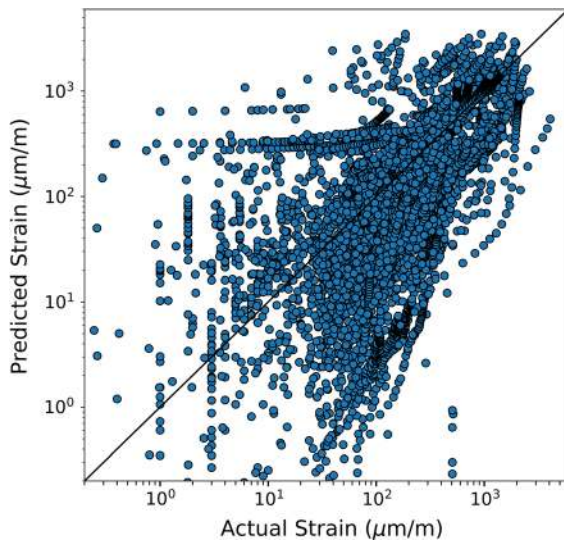
Fig. 4 The actual and predicted values for autogenous shrinkage model with swelling

reason, discussed in [96], is that the measurements of drying shrinkage often began with some unknown arbitrary delay rather than at the instant of exposure. A small delay can cause the swelling to appear as additional shrinkage (Fig. 3b).

Unfortunately, it is not feasible to calibrate k with the existing test data. Instead, the hydration model can be used to capture the swelling such as that considered in [96].

4.5 Prediction of autogenous shrinkage

The autogenous shrinkage can be calculated on the basis of concrete composition as

$$\epsilon_{au} = k_\gamma k_s C \left(\frac{t}{1 \text{ day}} \right)^n \tag{9}$$

Exponent n is calculated from Eq. (2), and parameters p and q from Eq. (3). Equation (4) for the prefactor is defined as

$$C = \frac{100}{(w/c)^{2.5} + \left(\frac{a/c}{10}\right)^{1.5}} \tag{10}$$

where parameter k_s takes into account the effects of the ratios of mass of silica fume (SiO_2) and of slag to the mass cement, per unit volume of concrete, and reads:

$$k_s = \left\{ 1 + 3 \left(\frac{SiO_2}{Cement} \right) \right\} \left\{ 1 + 2 \left(\frac{Slag}{Cement} \right) \right\} \tag{11}$$

The cement type factor k_γ is defined by Table 1. If the measurement record did not begin at the time of set, the unrecorded part must be subtracted as

$$\epsilon(t - t_s) = \epsilon(t) - \epsilon(t_s) \tag{12}$$

5 Alternative prefactor prediction from concrete strength

Formulas based on concrete composition alone have been inevitable for analyzing the entire NU database because the mean concrete strength f_c was not reported for about one-quarter of the lab tests. However, the required concrete strength f_c' prescribed by design codes, which is by about 8 MPa greater than the mean, f_c, is often the only concrete parameter specified in the design. So it is necessary to develop also alternative formula based on f_c'. For this purpose, exponent n is fixed at its average value, which is $n = 0.2$ (Fig. 2a). The prefactor has been recalibrated, accordingly, for this n value.

Both the autogenous shrinkage and the strength are controlled by the hydration reaction [70, 75, 97]. Since w/c is strongly correlated to strength, its effect need not be considered now. The same is true for the silica fume and for the equivalent age at different temperatures, for which similar strong correlations to strength exist. The effect of aggregate can be based on the formula of Pickett [98], which was justified by Hobbs [64] simplified analysis of an aggregate inclusion within a viscoelastic block of cement paste. This leads to the approximate formula [99]:

$$\epsilon_{au} = \epsilon_{au,p} (1 - g)^\alpha \tag{13}$$

where ϵ_{au} and $\epsilon_{au,p}$ are the autogenous shrinkage of concrete and of cement paste; and g = (volume of aggregates)/(volume of concrete). Pickett's formula is approximate but gave good results for the effect of aggregate content on shrinkage [20, 99]. Based on this formula,

$$C = k f_c (1 - g)^\alpha \tag{14}$$

Parameter $\alpha = 1.7$ gives the best overall fit for the NU

Fig. 5 The actual and
predicted values of
autogenous shrinkage in
linear and logarithmic scale
a, **b** composition based
model, **c**, **d** JSCE model, **e**,
f strength based model, **g**,
h Eurocode model and **k**,
l CEB MC90-99 model
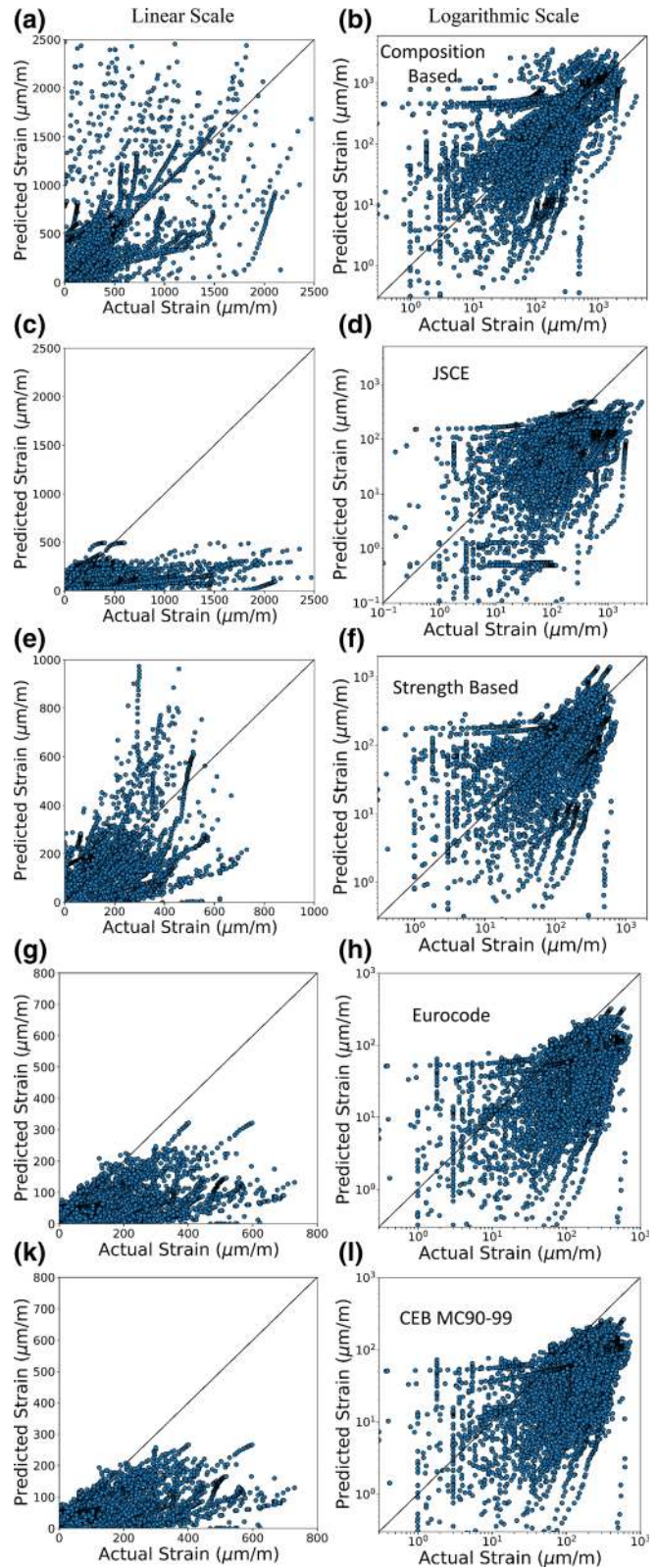
database. Calibration of parameter k with this database yields $k = 12$; so,

$$\epsilon_{au} = 12 f_c (1 - g)^{1.7} t^{0.2} \tag{15}$$

where as before, $\epsilon_{au} =$ autogenous shrinkage strain in $\mu m/m$; $f_c =$ mean compressive strength of concrete in MPa at 28 days of age, and $t =$ time after concrete set, in days. The formula also applies to cement paste, in which case $g = 0$. If g of concrete is not known, use $g = 0.7$ as default. There is no big need for parameters accounting for the temperature and age effects, since these effects are here approximately accounted for by means of f_c. In the case of water curing, as long as the specimen is under water, the autogenous shrinkage is not realized and should be subtracted. Also if the measurements start some time after the set, one must use the following equation to subtract the initial part of autogenous shrinkage curve;

$$\epsilon_{au}(t - t_s) = \epsilon_{au}(t) - \epsilon_{au}(t_s) \tag{16}$$

6 Verification of the model

It has long been advocated [78, 86, 87, 100, 101], and also endorsed in [102], that the verification of creep and shrinkage models must include both:

1. The optimum fitting of the *entire database* obtained by nonlinear regression, properly weighted to suppress data and sampling bias, with comparisons of the overall coefficients of variation of the prediction errors normalized by the mean of all data (and not the mean of errors), and
2. Similar comparisons of the prediction curves of the individual tests, in which case the random differences among various concretes are excluded and thus cannot obfuscate the trends.

Both methods are used here. To compare models, the unbiased coefficient of variation is calculated for each model as described in [86]. The specimens showing expansion had to be excluded since models did not consider initial swelling. Thus 230 tests remained to be used for comparisons.

The model of Tazawa and Miyazawa [46], recommended by the Standard Specification for Design and Construction of Concrete Structures by Japan Society

of Civil Engineers (JSCE 2002 model), is considered first. This version gave slightly better predictions than the 2007 one [39], so it considered here for the comparison. Its input parameters are the w/c and the cement type, and the final shrinkage is a function of w/c. The second model is that recommended by the European Committee for Standardization (Eurocode prEN [40]), which predicts the autogenous shrinkage from the 28-days compressive strength. The third is the CEB MC90 developed by Müller and Hilsdorf [41, 102, 103]. This model, revised in 1999 as CEB MC90-99, separates the total shrinkage into drying and autogenous parts. While the drying shrinkage has a similar form as in CEB MC90, this model introduced a separate formula predicting the autogenous shrinkage from the 28-days compressive strength and the cement type.

6.1 Model comparisons based on complete database

Most data points in the database are crowded in the short-time range (Fig. 5) while longtime data points are sparse. Ignoring it in calculating the coefficient of variation would introduce a severe bias against long times. To remedy it, we use an unbiased coefficient of variation, in which the time range is subdivided into 8 intervals of constant size in log-time and the data points are assigned weights inversely proportional to the number of points in each interval (Table 2), as proposed and used in [78, 86, 87, 100]. This is essential since the log-time intervals at short times have far more data points than those at long times. The data point weights, w_i, are

Table 2 Time intervals and interval weights

Interval (days)	Number of data points	Interval weight
0–1	416	0.052
1–4	460	0.047
4–16	829	0.026
16–64	989	0.022
64–256	688	0.031
256–1024	311	0.069
1024–4096	102	0.212
4096–16,384	40	0.540

$$w_i = \frac{1}{m_i \bar{w}} \quad \bar{w} = \sum_{i=1}^{n} \frac{1}{m_i} \qquad (17)$$

where n = number of all intervals and m_i = number of data points in the ith interval. The weighted standard deviation is for each model calculated as:

$$s = \sqrt{\frac{N}{N-p} \frac{\bar{w}}{n} \sum_{i=1}^{n} w_i \sum_{j=1}^{m} (\ln Y_{ij} - \ln y_{ij})^2} \qquad (18)$$

where N = number of all data points, y_{ij} = measured shrinkage data, Y_{ij} = corresponding model predictions, and p = number of free input parameters of the

Table 3 Unbiased CoV of predictive models

Model	Unbiased CoV	Number of tests fitted
Composition based formula	0.36	230
Strength based formula	0.37	172
JSCE	0.43	230
Eurocode	0.49	172
CEB MC90-99	0.49	172
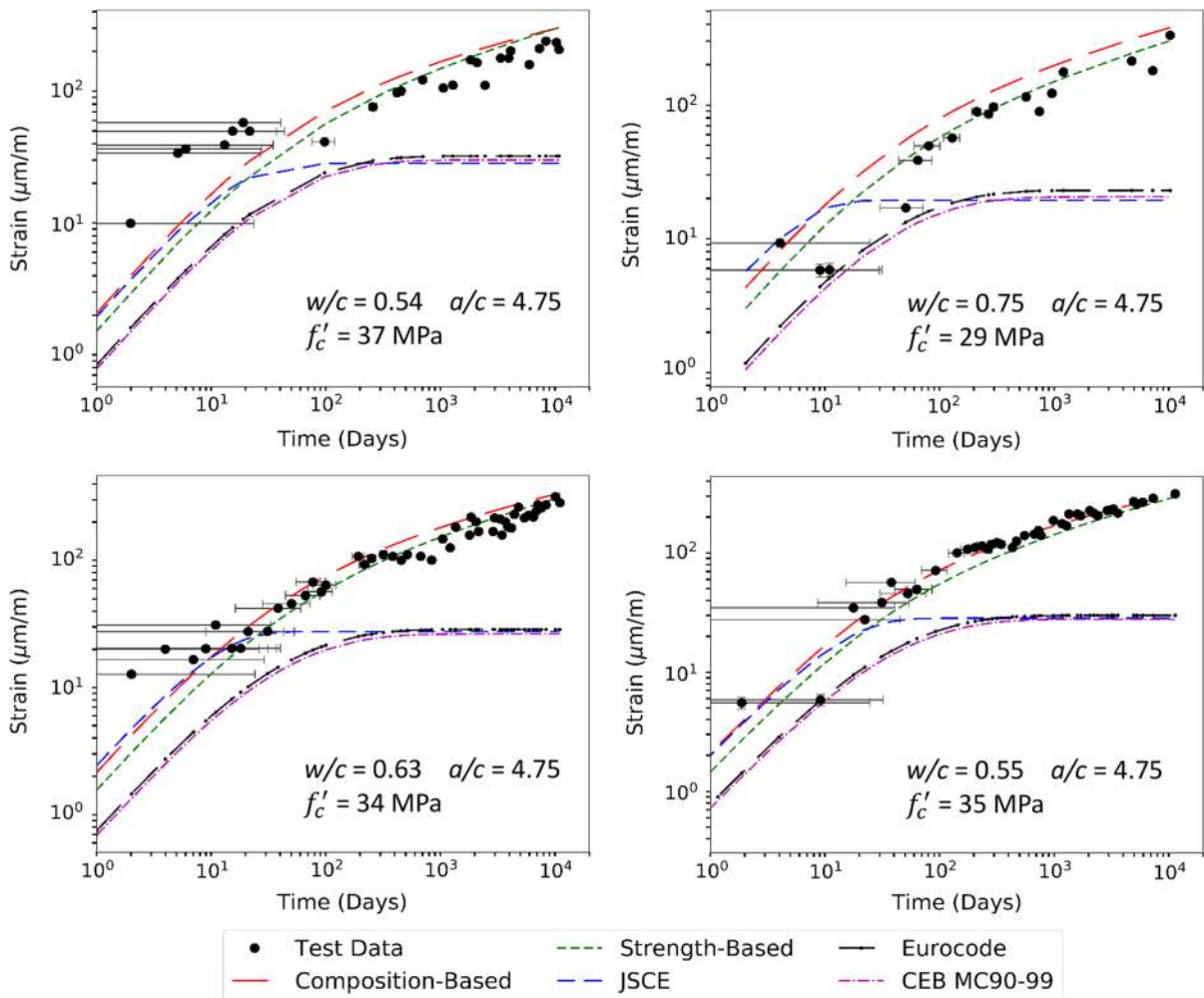
Fig. 6 Predictions compared to test data of Brooks

model (which must be subtracted from N to suppress bias). The standard deviation was calculated from the differences in the logarithms of the measurements and of data values. The reason is that what matters are not the absolute but the relative deviations (e.g., an error of 5 is small compared to 100 but large compared to 10). More fundamentally, the transformation from linear to logarithmic scale changes the data set from heteroscedastic to nearly homoscedastic. To get the coefficient of variation, ω, the standard deviation is divided by the weighted mean of all data points in the database;

$$\omega = \frac{s}{\bar{y}} \quad \bar{y} = \frac{\bar{w}}{n}\sum_{i=1}^{n} w_i \sum_{j=1}^{m_i} \ln y_{ij} \tag{19}$$

The calculated coefficients of variation seen in Table 3 document that the present model significantly improves predictions. The present composition-based model and the JSCE model, which require w/c and a/c as input, could be used to fit all of the 230 tests. For the tests which did not report the cement type, ordinary Portland cement was assumed. Among the 230 tests, 58 did not report the compressive strength, and so the present strength-based model could be used to fit only the remaining 172 tests. The JSCE model tends to better predict the autogenous shrinkage in early ages (low shrinkage values in Fig. 5) respect to the Eurocode and CEB models.

Figure 5 shows the prediction versus the reported values for the models (note that the range of axis is not the same in Fig. 5 as the composition-based model and the JSCE could fit more tests). The JSCE, Eurocode and CEB MC90-99 tend to underestimate most of the data points. One reason for the underestimation, especially for long times, is the incorrect final bound. The autogenous shrinkage strain tends to grow for years and probably decades, with no end in sight, while these models stop growth at almost only one month after setting. This general misconception has doubtless been caused by plotting the data in linear time scale. Also in linear scale time, error of the early data points can be many hours and an approach to a final asymptotic bound is an illusion. Another source of the error of these models is ignoring the effect of the aggregate content, whose increase greatly reduces autogenous shrinkage.

On the other hand, both present models can capture the data trend very well and show no systematic bias toward under- or over-prediction. Some, or much, of the large scatter seen in data could have been due to lack of precision in lab procedure or measurement. For many autogenous shrinkage tests, the sealing might not have been perfect and moisture loss might have occurred, which could have been detected by precision weighing of the specimens [48, 62]. Other sources of error could have been the lack of control on ambient temperature, certain chemicals, or reactive aggregates.
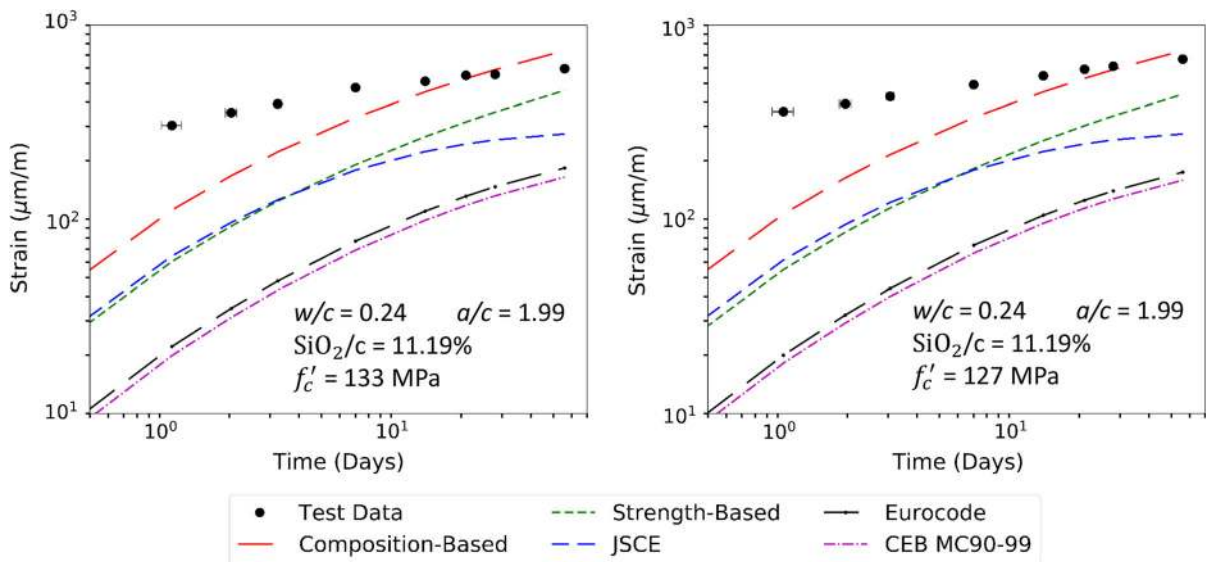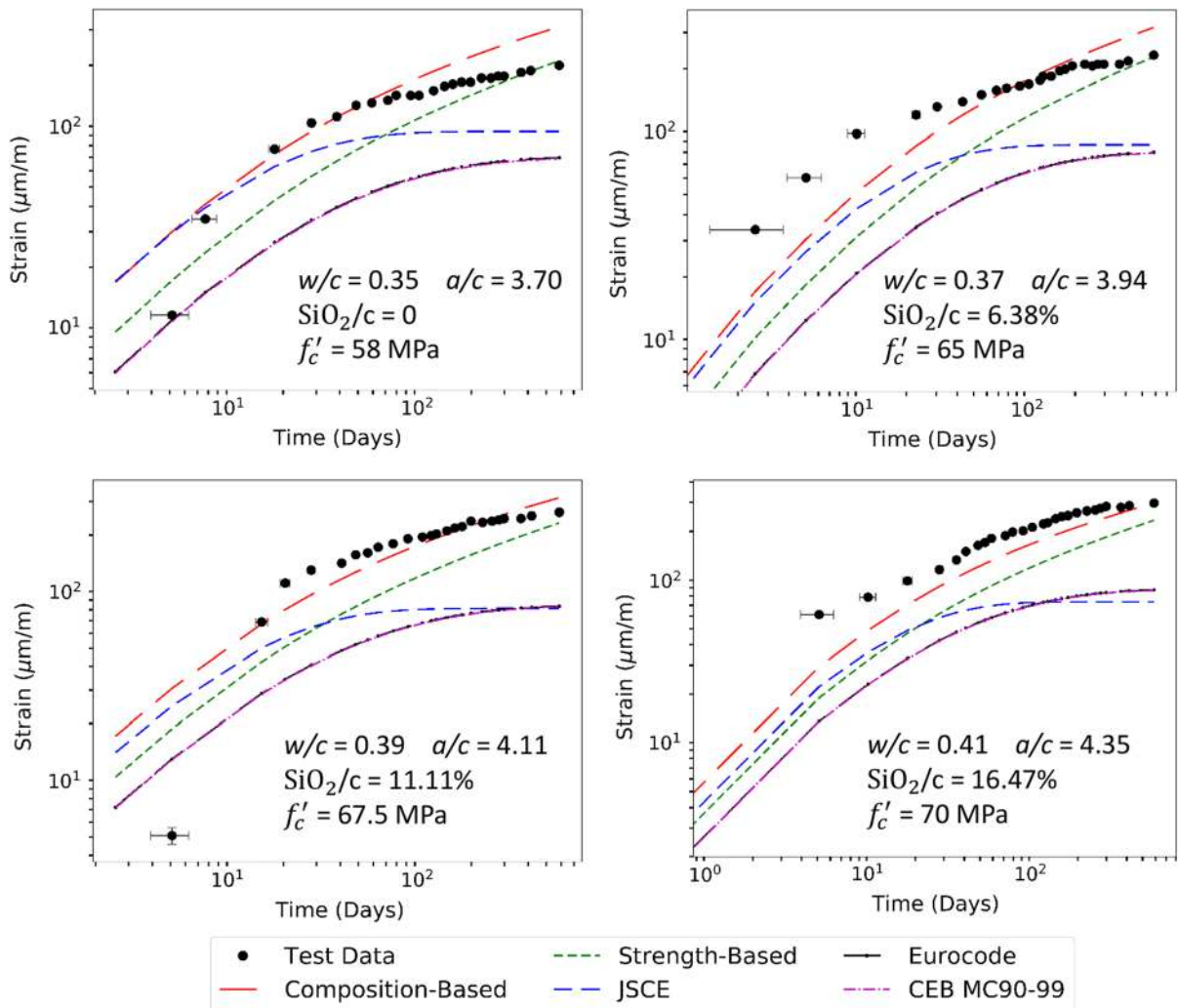

Fig. 7 Predictions compared to test data of Nakanishi

Fig. 8 Predictions compared to test data of Mazloom et al.

6.2 Predictions of various models for individual lab tests

For comparison, three data sets were selected which both the compressive strength and the concrete composition parameters have been reported. So, for these tests, it is possible to compare all the models. These three sets include 10 individual tests that are here selected so as to cover a wide range of compositions, strengths and test durations.

Set 1 In 1984, Brooks [85] reported a set of 36 shrinkage tests of which 18 were autogenous. The specimens were cylinders of radius 38 mm and height 255 mm, wet cured for 14 days. Figure 6 shows the predictions of all the models for the sample of four

specimens (the error bar shows uncertainty in recovering data).

Both present models gave better predictions than the previous ones. The time curves of all three models flatten too quickly and cannot capture the data trend seen in log-time scale. On the other hand, the presently proposed models capture the data trend satisfactorily.

Set 2 Nakanishi et al. [104] tested shrinkage of ten specimens, of which two were sealed. They were prisms with cross section 100×100 mm and height 400 mm, cured for one day, made with ordinary Portland cement and crushed sandstone, containing the same dosage of silica fume. Figure 7 shows the predictions of each model. The result of comparison is

the same with the previous case. Again, both present models gave better predictions than the others.

Set 3 Mazloom et al. [95] tested shrinkage of four sealed specimens, shown in Fig. 8. They were cylinders of radius 40 mm and height 270 mm, wet cured for the periods of 7 days. The present composition-based formula gave excellent fits, while the other models underestimated the observed shrinkage.

The present composition-based model correctly captures the magnitude and evolution of the shrinkage curve. The European models usually underestimate the autogenous shrinkage for the North American concretes. Part of the reason could be that the European models were calibrated for European concretes, which generally show lower autogenous shrinkage [102]. The underestimation of the JSCE model is due to incorrect evolution shape of shrinkage curve. The JSCE function first rises fast and then flattens quickly. So, if the measurements begin after the curing period, the JSCE function does not show much of shrinkage. Also, the assumption of a horizontal asymptote for shrinkage caused the models to underestimate the long-term shrinkage. The proposed models showed good predictions for both short and long term. The JSCE model is insensitive to silica fume, which may explain the underestimation for specimens with silica fume content.

7 Conclusions

1. The autogenous shrinkage, driven by the hydration reaction, continues at a decaying rate for decades of years. The existing test data give no sign of approach to a finite asymptotic bound.
2. From hours up to decades of years, the autogenous shrinkage evolution is well approximated by a power law of the time, whose exponent is roughly 0.2.
3. Among the material composition factors, the water-cement and aggregate-cement ratios are the most important influencing factors. Further ones are the type and fineness of cement, additives such as blast-furnace slag and silica fume, and the type of curing (in fog or underwater).
4. Instead of the aforementioned composition factors the factors that can predict autogenous shrinkage almost equally well are the 28-days compressive strength of concrete, and the volume fraction of aggregate.
5. In data evaluations, the bias due to crowding of test data at short times, and to differences in the time ranges and the numbers of data reported by various experimenters, must be eliminated by proper weighting in the statistical regression.

Closing comment Finally it is emphasized that, in presence of external drying and creep due to applied load, accurate predictions will require treating the autogenous shrinkage as a consequence of pore humidity drop caused jointly by self-desiccation due to hydration and moisture diffusion. This will require considering the time evolution of humidity profiles.

Compliance with ethical standards

Conflict of interest The authors declare that they have no conflict of interest.

References

1. Bažant ZP, Hubler MH, Yu Q (2011) Excessive creep deflections: an awakening. Concr Int 33(8):44–46
2. Bažant ZP, Hubler MH, Yu Q (2011) Pervasiveness of excessive segmental bridge deflections: wake-up call for creep. ACI Struct J 108(6):766
3. Bažant ZP, Jirásek M, Hubler M, Carol I (2015) RILEM draft recommendation: TC-242-MDC multi-decade creep and shrinkage of concrete: material model and structural analysis Model B4 for creep, drying shrinkage and autogenous shrinkage of normal and high-strength concretes

with multi-decade applicability. Mater Struct 48(4):753–770

4. Bažant ZP, Yu Q, Li G-H (2012) Excessive long-time deflections of prestressed box girders. I: Record-span bridge in Palau and other paradigms. J Struct Eng 138(6):676–686

5. Bažant Z, Najjar L (1972) Nonlinear water diffusion in nonsaturated concrete. Matériaux et Construction 5(1):3–20

6. Rahimi-Aghdam S, Bažant ZP, Qomi MA (2017) Cement hydration from hours to centuries controlled by diffusion through barrier shells of CSH. J Mech Phys Solids 99:211–224

7. Rahimi-Aghdam S, Rasoolinejad M, Bažant ZP (2019) Moisture Diffusion in Unsaturated Self-Desiccating Concrete with Humidity-Dependent Permeability and Nonlinear Sorption Isotherm. J Eng Mech 145(5):04019032

8. Baroghel-Bouny V, Mounanga P, Khelidj A, Loukili A, Rafai N (2006) Autogenous deformations of cement pastes: part II. W/C effects, micro–macro correlations, and threshold values. Cem Concr Res 36(1):123–136

9. Rasoolinejad M, Rahimi-Aghdam S, Bažant ZP (2018) Statistical filtering of useful concrete creep data from imperfect laboratory tests. Mater Struct 51(6):153

10. Lynam CG (1934) Growth and movement in Portland cement concrete. Oxford University Press, London

11. Davis HE (1940) Autogenous volume change of concrete. Proc ASTM 40:1103–1110

12. Jensen OM, Hansen PF (2001) Autogenous deformation and RH-change in perspective. Cem Concr Res 31(12):1859–1865

13. Tazawa E-I (2014) Autogenous shrinkage of concrete. CRC Press, Boca Raton

14. Holt EE (2001) Early age autogenous shrinkage of concrete, vol 446. Technical Research Centre of Finland, Espoo

15. Tazawa E-I, Miyazawa S, Kasai T (1995) Chemical shrinkage and autogenous shrinkage of hydrating cement paste. Cem Concr Res 25(2):288–292

16. Gawin D, Pesavento F, Schrefler BA (2006) Hygro-thermo-chemo-mechanical modelling of concrete at early ages and beyond. Part I: Hydration and hygro-thermal phenomena. Int J Numer Methods Eng 67(3):299–331

17. Grasley ZC, Leung CK (2011) Desiccation shrinkage of cementitious materials as an aging, poroviscoelastic response. Cem Concr Res 41(1):77–89

18. Hua C, Acker P, Ehrlacher A (1995) Analyses and models of the autogenous shrinkage of hardening cement paste: I. Modelling at macroscopic scale. Cem Concr Res 25(7):1457–1468

19. Luan Y, Ishida T (2013) Enhanced shrinkage model based on early age hydration and moisture status in pore structure. J Adv Concr Technol 11(12):360–373

20. Lura P, Jensen OM, van Breugel K (2003) Autogenous shrinkage in high-performance cement paste: an evaluation of basic mechanisms. Cem Concr Res 33(2):223–232

21. Bažant ZP, Donmez A (2016) Extrapolation of short-time drying shrinkage tests based on measured diffusion size effect: concept and reality. Mater Struct 49(1–2):411–420

22. Dönmez A, Bažant ZP (2016) Shape factors for concrete shrinkage and drying creep in model B4 refined by nonlinear diffusion analysis. Mater Struct 49(11):4779–4784

23. Bentz DP (1997) Three-dimensional computer simulation of Portland cement hydration and microstructure development. J Am Ceram Soc 80(1):3–21

24. Bentz DP, Garboczi EJ (1990) Digitised simulation model for microstructural development. Ceram Trans 16:211–226

25. Di Luzio G, Cusatis G (2009) Hygro-thermo-chemical modeling of high performance concrete. I: Theory. Cem Concr Compos 31(5):301–308

26. Di Luzio G, Cusatis G (2009) Hygro-thermo-chemical modeling of high-performance concrete. II: Numerical implementation, calibration, and validation. Cem Concr Compos 31(5):309–324

27. Jennings HM, Johnson SK (1986) Simulation of microstructure development during the hydration of a cement compound. J Am Ceram Soc 69(11):790–795

28. Lin F, Meyer C (2009) Hydration kinetics modeling of Portland cement considering the effects of curing temperature and applied pressure. Cem Concr Res 39(4):255–265

29. Navi P, Pignat C (1996) Simulation of cement hydration and the connectivity of the capillary pore space. Adv Cem Based Mater 4(2):58–67

30. Pathirage M, Bentz DP, Di Luzio G, Masoero E, Cusatis G (2018) A multiscale framework for the prediction of concrete self-desiccation. In: Computational modelling of concrete structures: proceedings of the conference on computational modelling of concrete and concrete structures (EURO-C 2018), Feb 26–March 1, 2018, Bad Hofgastein, Austria. CRC Press, pp 203

31. Nishiyama M (2009) Mechanical properties of concrete and reinforcement. J Adv Concr Technol 7(2):157–182

32. Holt E, Leivo M (2004) Cracking risks associated with early age shrinkage. Cem Concr Compos 26(5):521–530

33. Schiessl P, Beckhaus K, Schachinger I, Rucker P (2004) New results on early-age cracking risk of special concrete. Cem Concr Aggreg 26(2):1–9

34. Sellevold E (1994) High performance concrete: early volume change and cracking tendency. In: Thermal cracking in concrete at early ages, pp 229–236

35. Tazawa E (1992) Autogeneous shrinkage caused by self desiccation in cementitious material. In: 9th International congress on the chemistry of cement, New Delhi, pp 712–718

36. Ziegeldorf S, Müller H, Plöhn J, Hilsdorf H (1982) Autogenous shrinkage and crack formation in young concrete. In: International conference on concrete of early ages, pp 83–88

37. Igarashi S, Bentur A, Kovler K (1999) Stresses and creep relaxation induced in restrained autogenous shrinkage of high-strength pastes and concretes. Adv Cem Res 11(4):169–177

38. Shah SP, Weiss WJ, Yang W (1998) Shrinkage cracking-can it be prevented? Concr Int 20(4):51–55

39. Japan Society of Civil Engineers (JSCE) (2007) Standard specification for concrete structures. Structural performance verification

40. Comité Européen de Normalisation (2004) Design of concrete structurespart 1-1: general rules and rules for buildings. Eurocode 2, EN 1992-1-1: 2004: E

41. Fédération Internationale Du Béton (1999) Structural concrete: textbook on behaviour, design and performance: updated knowledge of the CEB/FIP Model Code 1990

42. Beverly P (2013) Fib model code for concrete structures 2010. Ernst & Sohn, Hoboken

43. Neville AM (1995) Properties of concrete, vol 4. Longman, London

44. Swayze M (1960) Discussion on: Volume changes of concrete. In: Proceedings of 4th international symposium on the chemistry of cement, pp 700–702

45. Bennett E, Loat D (1970) Shrinkage and creep of concrete as affected by the fineness of Portland cement. Mag Concr Res 22(71):69–78

46. Miyazawa S, Tazawa E (2005) Prediction model for autogenous shrinkage of concrete with different type of cement. In: Proceedings of the fourth international research seminar, Gaithersburg, Maryland, USA

47. Tazawa E-I, Miyazawa S (1995) Influence of cement and admixture on autogenous shrinkage of cement paste. Cem Concr Res 25(2):281–287

48. Eppers S, Muller C (2008) Autogenous shrinkage strain of ultra-high-performance concrete (UHPC). In: Proceeding of the 2nd international symposium on ultra high performance concrete. Kassel University Press, Kassel, pp 433–441

49. Jensen M, Hansen PF (1996) Autog enous deformation and change of the relative humidity in silica fume-modified cement paste. Mater J 93(6):539–543

50. Jensen OM, Hansen PF (1995) Autogenous relative humidity change in silica fume-modified cement paste. Adv Cem Based 7(25):33–38

51. Persson B (1997) Self-desiccation and its importance in concrete technology. Mater Struct 30(5):293–305

52. Zhang M, Tam C, Leow M (2003) Effect of water-to-cementitious materials ratio and silica fume on the autogenous shrinkage of concrete. Cem Concr Res 33(10):1687–1694

53. Buil M, Delage P (1987) Some further evidence on a specific effect of silica fume on the pore structure of Portland cement mortars. Cem Concr Res 17(1):65–69

54. Igarashi S-I, Watanabe A, Kawamura M (2005) Evaluation of capillary pore size characteristics in high-strength concrete at early ages. Cem Concr Res 35(3):513–519

55. Meddah MS, Tagnit-Hamou A (2009) Pore structure of concrete with mineral admixtures and its effect on self-desiccation shrinkage. Mater J 106(3):241–250

56. Jiang Z, Sun Z, Wang P (2005) Autogenous relative humidity change and autogenous shrinkage of high-performance cement pastes. Cem Concr Res 35(8):1539–1545

57. Lee K, Lee H, Lee S, Kim G (2006) Autogenous shrinkage of concrete containing granulated blast-furnace slag. Cem Concr Res 36(7):1279–1285

58. Tazawa E, Miyazawa S (1997) Influence of constituents and composition on autogenous shrinkage of cementitious materials. Mag Concr Res 49(178):15–22

59. Eppers S, Mueller C (2007) On the examination of the autogenous shrinkage cracking propensy by means of the restrained ring test with particular consideration of the temperature influences. VDZ concrete technology reports, 2009, pp 57–70

60. Yan P, Chen Z, Wang J, Zheng F (2007) Autogenous shrinkage of concrete prepared with the binders containing different kinds of mineral admixture. In Proceedings of the 12th international conference on chemistry of cement, Canada

61. Feldman RF (1983) Significance of porosity measurements on blended cement performance. Spec Publ 79:415–434

62. Staquet S, Espion B (2004) Evolution of the thermal expansion coefficient of UHPC incorporating very fine fly ash and metakaolin. In: International RILEM symposium on concrete science and engineering: a tribute to Arnon Bentur. RILEM Publications SARL

63. Khayat K, Mitchell D (2009) Self-consolidating concrete for precast, prestressed concrete bridge elements, vol 628. Transportation Research Board, Washington, DC

64. Hobbs D (1974) Influence of aggregate restraint on the shrinkage of concrete. J Proc 71(9):445–450

65. Shah SP, Ahmad SH (1994) High performance concrete. Properties and applications. McGraw-Hill, New York

66. Bjøntegaard Ø, Hammer T, Sellevold EJ (2004) On the measurement of free deformation of early age cement paste and concrete. Cem Concr Compos 26(5):427–435

67. Jensen OM, Hansen PF (1999) Influence of temperature on autogenous deformation and relative humidity change in hardening cement paste. Cem Concr Res 29(4):567–575

68. Loukili A, Chopin D, Khelidj A, Le Touzo J-Y (2000) A new approach to determine autogenous shrinkage of mortar at an early age considering temperature history. Cem Concr Res 30(6):915–922

69. Kamen A, Denarie E, Brühwiler E (2007) Thermal effects on physico-mechanical properties of ultra-high-performance fiber-reinforced concrete. ACI Mater J 104(4):415

70. Staquet S, Boulay C, DAloïa L, Toutlemonde F (2006) Autogenous shrinkage of a self-compacting VHPC in isothermal and realistic temperature conditions. In: 2nd International RILEM symposium on advances in concrete through science and engineering, pp 361. RILEM Publications SARL

71. Turcry P, Loukili A, Barcelo L, Casabonne JM (2002) Can the maturity concept be used to separate the autogenous shrinkage and thermal deformation of a cement paste at early age? Cem Concr Res 32(9):1443–1450

72. Baroghel-Bouny V, Mounanga P, Loukili A, Khelidj A (2004) From chemical and microstructural evolution of cement pastes to the development of autogenous deformations. Spec Publ 220:1–22

73. Bjøntegaard Ø, Sellevold E (2001) Interaction between thermal dilation and autogenous deformation in high performance concrete. Mater Struct 34(5):266–272

74. Lura P, van Breugel K (2003) Effect of curing temperature on autogenous deformations of cement paste and high performance concrete for different cement types. In: 11th International congress on the chemistry of cement: proceedings, South Africa, pp 1616–1625

75. Mounanga P, Baroghel-Bouny V, Loukili A, Khelidj A (2006) Autogenous deformations of cement pastes: part I.

Temperature effects at early age and micro–macro correlations. Cem Concr Res 36(1):110–122

76. Mounanga P, Loukili A, Bouasker M, Khelidj A, Coué R (2006) Effect of setting retarder on the early age deformations of self-compacting mortars. In: International RILEM conference on volume changes of hardening concrete: testing and mitigation, pp 311–320. RILEM Publications SARL

77. Persson B (2005) On the temperature effect on self-desiccation of concrete. In: Proceedings of the 4th international research seminar on self-desiccation and its importance in concrete technology, Gaithersburg, Maryland, USA. Division Building Materials, Lund Institute of Technology, Lund, Sweden, pp 101–124

78. Bažant ZP, Baweja S (1995) Justification and refinements of model B3 for concrete creep and shrinkage 1. statistics and sensitivity. Mater Struct 28(7):415–430

79. Collins TM (1989) Proportioning high-strength concrete to control creep and shrinkage. Mater J 86(6):576–580

80. Bažant Z, Panula L (1978) Practical prediction of time-dependent deformations of concrete. Matériaux et Construction 11(5):317–328

81. Bažant ZP, Li G-H (2008) Comprehensive database on concrete creep and shrinkage. ACI Mater J 105(6):635–637

82. Hubler MH, Wendner R, Bažant ZP (2015) Comprehensive database for concrete creep and shrinkage: analysis and recommendations for testing and recording. ACI Mater J 112(4):547

83. Wendner R, Hubler MH, Bažant ZP (2015) Optimization method, choice of form and uncertainty quantification of model B4 using laboratory and multi-decade bridge databases. Mater Struct 48(4):771–796

84. Troxell G (1958) Log-time creep and shrinkage tests of plain and reinforced concrete. ASTM 58:1101–1120

85. Brooks J (2000) Elasticity, creep, and shrinkage of concretes containing admixtures. Spec Publ 194:283–360

86. Bažant ZP, Li G-H (2008) Unbiased statistical comparison of creep and shrinkage prediction models. ACI Mater J 105(6):610

87. Bažant ZP, Jirásek M (2018) Creep and hygrothermal effects in concrete structures, vol 225. Springer, Berlin

88. Bažant ZP, Rahimi-Aghdam S (2016) Diffusion-controlled and creep-mitigated ASR damage via microplane model. I: Mass concrete. J Eng Mech 143(2):04016108

89. Rahimi-Aghdam S, Bažant ZP, Caner FC (2016) Diffusion-controlled and creep-mitigated ASR damage via microplane model. II: Material degradation, drying, and verification. J Eng Mech 143(2):04016109

90. Hubler MH, Wendner R, Bažant ZP (2015) Statistical justification of model B4 for drying and autogenous shrinkage of concrete and comparisons to other models. Mater Struct 48(4):797–814

91. Bažant Z, Dönmez A, Masoero E, Aghdam SR (2015) Interaction of concrete creep, shrinkage and swelling with water, hydration, and damage: nano-macro-chemo. In: CONCREEP 10. ASCE, Washington, DC, pp 1–12

92. Loukili A, Khelidj A, Richard P (1999) Hydration kinetics, change of relative humidity, and autogenous shrinkage of ultra-high-strength concrete. Cem Concr Res 29(4):577–584

93. Persson B (2002) Eight-year exploration of shrinkage in high-performance concrete. Cem Concr Res 32(8):1229–1237

94. Rahimi-Aghdam S, Bažant ZP, Cusatis G (2018) Extended microprestress-solidification theory for long-term creep with diffusion size effect in concrete at variable environment. J Eng Mech 145(2):04018131

95. Mazloom M, Ramezanianpour A, Brooks J (2004) Effect of silica fume on mechanical properties of high-strength concrete. Cem Concr Compos 26(4):347–357

96. Rahimi-Aghdam S, Masoero E, Rasoolinejad M, Bažant ZP (2019) Century-long expansion of hydrating cement counteracting concrete shrinkage due to humidity drop from selfdesiccation or external drying. Mater Struct 52(1):11

97. Ulm F-J, Coussy O (1996) Strength growth as chemoplastic hardening in early age concrete. J Eng Mech 122(12):1123–1132

98. Pickett G (1956) Effect of aggregate on shrinkage of concrete and a hypothesis concerning shrinkage. J Proc 52(1):581–590

99. Grasley Z, Lange D, Brinks A, DAmbrosia M (2005) Modeling autogenous shrinkage of concrete accounting for creep caused by aggregate restraint. In: Proceedings of the 4th international seminar on self-desiccation and its importance in concrete technology, NIST, Gaithersburg, MD, pp 78–94

100. Bažant ZP, Panula L (1980) Creep and shrinkage characterization for analyzing prestressed concrete structures. PCI J 25(3):86–122

101. Bažant ZP, Yu Q (2005) Designing against size effect on shear strength of reinforced concrete beams without stirrups: II. Verification and calibration. J Struct Eng 131(12):1886–1897

102. Videla C, Carreira DJ, Garner N et al (2008) Guide for modeling and calculating shrinkage and creep in hardened concrete. ACI report, p 209

103. Comite Euro International du Beton (1993) CEB-FIP Model Code 1990. Thomas Telford Publishing. https://doi.org/10.1680/ceb-fipmc1990.35430

104. Nakanishi H, Tamaki S, Yaguchi M, Yamada K, Kinoshita M, Ishimori M, Okazawa S (2003) Performance of a multifunctional and multipurpose superplasticizer for concrete. Spec Publ 217:327–342